# *Communications*

## Synthesis of Platinum Y-Junction Nanostructures Using Hierarchically Designed Alumina Templates and Their Enhanced Electrocatalytic Activity for Fuel-Cell Applications†

Subhramannia Mahima,‡ Ramaiyan Kannan,‡ Indulekha Komath,‡ Mohammed Aslam,§ and Vijayamohanan K. Pillai*,‡

*Physical and Materials Chemistry Division, National Chemical Laboratory, Pune 411008, India, and Department of Materials Science and Engineering and the International Institute for Nanotechnology, Northwestern University, Evanston, Illinois 60208*

*Received July 30, 2007*
*Revised Manuscript Received October 31, 2007*

Recently, much effort has been directed toward the fabrication of shape-selective nanostructures because of their exquisite size and shape-dependent properties and their technological relevance in diverse areas such as catalysis, photochemistry, chemical sensors, and optoelectronics.[1] These nanostructures are generally synthesized in many forms, including highly monodispersed spherical nanoparticles to several anisotropic nanostructures such as wires/rods, tubes, and ribbons.[2] It is generally accepted that the morphology of a nanostructure could be remarkably tuned during the synthesis by controlling pertinent parameters such as temperature, nature of surfactant, metal ion to capping molecule ratio, and the concentration of other additives in order to control the physical and chemical properties of these materials.[3] As a result, various methods have been developed to generate many of these nanolevel architectures with good shape control.[4] Among these, the template-assisted route has been one of the widely investigated and exploited approaches, because it provides several distinct advantages over other approaches. More importantly, it offers a convenient route to precisely control the dimension of the nanostructures, and these structures can be released easily from the support.[5] Templates that can be used include soft (such as micelles) as well as hard (such as porous polymeric membrane, anodic alumina membrane) templates.[6] In particular, hard templates, like porous anodic alumina membrane (PAAM), have been extensively used because of many desirable characteristics, including tunable pore dimensions and lengths, good mechanical and thermal stability, and well-developed fabrication methods.[7] Although processing inside these type of porous templates is ideal to produce uniform morphologies, this route has been accomplished to date successfully only for linear structures. Interestingly, fabrication of three terminal morphology like Y-junctions are potentially promising for the development of molecular-scale electronic devices.[8]However, the fabrication of these junctions are difficult to achieve using conventional methods because the linear structure cannot be controllably altered along its length. Consequently, various ideas for postgrowth modifications have been attempted, including electron beam welding to form molecular junctions,[9] although these have been hard to implement and are prone to create defects.

In this communication, we report the first example of the fabrication of Y-shaped platinum nanostructures. Platinum has been selected because of its outstanding role as multifunctional catalysts in many industrial applications, particularly in fuel cells.[10]We use PAAM with controlled branching to grow individual Y-junction platinum nanostructures via

* Corresponding author. E-mail: vk.pillai@ncl.res.in.
† Part of the "Templated Materials Special Issue".
‡ National Chemical Laboratory.
§ Northwestern University.

(1) (a) Hirai, H.; Wakabayashi, H.; Komiyama, M. *Chem. Lett.* **1983**, 1047. (b) Brugger, P. A.; Cuendet, P.; Gratzel, M *J. Am. Chem. Soc.* **1981**, *103*, 2923. (c) Thomas, J. M *Pure Appl. Chem.* **1988**, *60*, 1517. (d) Schon, G.; Simon, U. *Colloid Polym. Sci.* **1995**, *273*, 202.

(2) (a) Turkevich, J *Discuss. Faraday Soc* **1951**, *11*, 55. (b) Finke, R. G. In *Metal Nanoparticles: Synthesis, Characterization, and Applications*; Feldheim, D. L., Foss, C. A., Jr., Eds.; Marcel Dekker, New York, 2002, 17. (c) Schwartzberg, A. M.; Olson, T. Y.; Talley, C. E.; Zhang, J. Z *J. Phys. Chem. B* **2006**, *110*, 19935. (d) Sau, T. K.; Murphy, C. J *J. Am. Chem. Soc.* **2004**, *126*, 8648. (e) Widegren, J. A.; Aiken, J. D.; Ozkar, S.; Finke, R. G *Chem. Mater.* **2001**, *13*, 312. (f) Zhao, Y.; Guo, Y.-G.; Zhang, Y.-L.; Jiao, K *Phys. Chem. Chem. Phys.* **2004**, *6*, 1766. (g) Melosh, N. A.; Doukai, A.; Diana, F.; Gerardot, B.; Badolato, A.; Petroff, P. M.; Heath, J. R. *Science* **2003**, *300*, 112. (h) Xiao, Z.-L.; Han, C. Y.; Kwok, W.-K.; Wang, H.-H.; Welp, U.; Wang, J.; Crabtree, G. W *J. Am. Chem. Soc.* **2004**, *126*, 2316. (i) Shirai, M.; Igeta, K.; Arai, M. *Chem. Commun.* **2000**, 623.

(3) (a) Lifshitz, E.; Bashouti, M.; Kloper, V.; Kigel, A.; Eisen, M. S.; Berger, S *Nano Lett.* **2003**, *3*, 857. (b) Zhou, G.; Lu, M.; Xiu, Z.; Wang, S.; Zhang, H.; Zhou, Y.; Wang, S. *J. Phys. Chem. B* **2006**, *110*, 6543. (c) Chen, J.; Herricks, T.; Xia, Y. *Angew. Chem., Int. Ed.* **2005**, *44*, 2589.

(4) (a) Martin, C. R *Chem. Mater.* **1996**, *8*, 1739. (b) Yang, C.-M.; Weidenthaler, C.; Spliethoff, B.; Mayanna, M.; Schuth, F *Chem. Mater.* **2005**, *17*, 355. (c) Duan, X. F.; Lieber, C. M. *Adv. Mater.* **2000**, *12*, 298. (d) Manna, L.; Scher, E. C.; Alivisators, A. P *J. Am. Chem. Soc.* **2000**, *122*, 12700. (e) Lifshitz, E.; Bashouti, M.; Kloper,V.; Kigel, A. M.; Eisen, S.; Berger, S *Nano Lett.* **2003**, *3*, 857. (f) Zhou, G.; Lu, M.; Xiu, Z.; Wang, S.; Zhang, H.; Zhou, Y.; Wang, S. *J. Phys. Chem. B* **2006**, *110*, 6543. (g) Chen, J.; Herricks, T.; Xia, Y. *Angew. Chem., Int. Ed.* **2005**, *44*, 2589.

(5) (a) Hulteen, J. C.; Martin, C. R. *J. Mater. Chem.* **1997**, *7*, 1075. (b) Ou, F. S.; Shaijumon, M. M.; Ci, L.; Benicewicz, D.; Vajtai, R.; Ajayan, P. M. *Appl. Phys. Lett.* **2006**, *89*, 243122.

(6) Zhang, D.; Qi, L.; Yang, J.; Ma, J.; Cheng, H.; Huang, L. *Chem. Mater.* **2004**, *16*, 872.

(7) (a) Masuda, H.; Hasegwa, F.; Ono, S *J. Electrochem. Soc.* **1997**, *144*, 127. (b) Li, A. P.; Muller, F.; Birner, A.; Nielsch, K.; Gosele, U *J. Appl. Phys.* **1998**, *84*, 6023. (c) Jessensky, O.; Muller, F.; Gosele, U. *Appl. Phys. Lett.* **1998**, *72*, 1173.

(8) (a) Papadopoulos, C.; Rakitinv, A.; Liv, J.; Vedeneev, A. S.; Xu, J. M *Phys. Rev. Lett.* **2000**, *85*, 3476. (b) Tian, Y.; Meng, G.; Biswas, S. K.; Ajayan, P. M.; Sun, S.; Zhang, L *Appl. Phys. Lett.* **2004**, *85*, 967. (c) Zach, M. P.; Ng, K. H.; Penner, R. M. *Science* **2000**, *290*, 2120.

(9) Terrones, M.; Banhart, F.; Grobert, N.; Charlier, J.-C.; Terrones, H.; Ajayan, P. M *Phys. Rev. Lett.* **2002**, *89*, 075505.

(10) (a) Girishkumar, G.; Rettker, M.; Underhile, R.; Binz, D.; Vinodgopal, K.; McGinn, P.; Kamat, P *Langmuir* **2005**, *21*, 8487. (b) Xiong, L.; Manthiram, A. *Electrochim. Acta* **2005**, *50*, 3200. (c) Williams, K. R.; Burstein, G. T. *Catal. Today* **1997**, *38*, 401.

10.1021/cm702102b CCC: $40.75 
Published on Web 11/30/2007

an electrochemical route. Although a few reports are available on the formation of Y-junction carbon nanotubes,[11] only limited progress has been made to date on the synthesis of metallic Y-junction or branched nanostructures.[8b,12] For example, Choi et al. have reported the fabrication of hierarchically ordered branched silver nanowires using PAAM.[12b] Our Pt Y-junctions show unique electrocatalytic activity for formic acid and ethanol oxidation (two important reactions for microfuel cells) in comparison with that of commercial platinized carbon and nanowires of platinum.

Scanning electron micrographs (SEM) of the anodic aluminum oxide template with Y-branched nanochannels (cross-sectional view; shown in the Supporting Information, Figure SI-1) have been fabricated via an extended two-step anodization as reported elsewhere.[8b,11b] (experimental details in the Supporting Information) Close examination of the micrograph reveals Y-branched nanochannels with stems and branches of about 100 and 50 nm diameters, respectively. Furthermore, the angle between the two branches is about 8°, as shown in the micrograph, although these parameters could be controlled systematically by varying temperature, anodization time, and nature and concentration of the electrolyte.

A typical field-emission scanning electron micrograph (FESEM) of the top view of the Pt Y-junction nanostructures (before dissolving the membrane), prepared using the above hierarchically designed alumina template, is shown in Figure 1a, where the image reveals that almost all the pores are effectively filled with Pt (experimental details in the Supporting Information). Further, FESEM image of Pt Y-junction nanostructure after dissolving the membrane in 0.1 M NaOH is shown in Figure 1b−d, where the images clearly reveal uniform Y-junctions with well-defined branches and stems having diameter ca. 100 and 50 nm, respectively, in close agreement with those of the Y-branched alumina nanochannels. In addition, the angle between the branches is ca. 12°, slightly higher compared to that of the template, perhaps because of the tendency of the structure to release the strain involved at the junction after the dissolution of the membrane. Also, Figure 1e shows the SEM image of some broken Y-junction nanostructures, presumably formed during purification. In addition, the energy-dispersive X-ray analysis (EDX) spectrum is shown in Figure 1f, which confirms the complete removal of Al from the sample (Si peak seen in the spectrum, could be from the substrate).

Because these Y-junction nanostructures of platinum are obtained only after maintaining the electrolyte bath at 80 °C for 30 min, we have further carried out templated electrodeposition under different conditions, in order to understand the effect of temperature. Interestingly, at room temperature and at 60 °C, SEM images (not shown for brevity) reveal only tiny nanorods of Pt, and hence it is absolutely essential to maintain the bath at a higher temperature like 80 °C to form Y-junctions. This is because the nanoporous structure of the template, because of its slow diffusion (Knudsen diffusion), hinders the deposition rate, which in turn prevents uniformity and quality of the structure at low temperature. At higher temperature, the mass-transfer resistance is reduced by decreasing the Nernst diffusion layer thickness, which facilitates the Y-junction formation. In contrast, reports are available on the utilization of ultrasonication during template-assisted electrodeposition to improve mass-transfer resistance.[13]

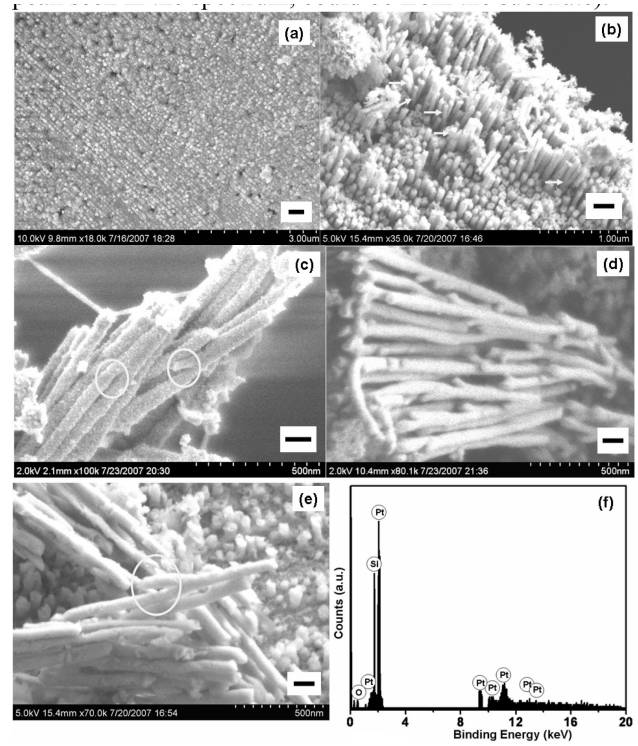


**Figure 1.** FESEM image of Pt Y-junction nanostructure (a) before dissolving the membrane (top view; scale bar 300 nm); (b−d) after etching the alumina template in 0.1 M NaOH, where the diameter of the stem and branches are ca. 100 and 50 nm, respectively (scale bar 200, 100, and 100 nm, respectively); (e) some broken Y-junction nanostructures (scale bar 100 nm); figure (f) shows the EDX spectrum taken from the Pt Y-junction.

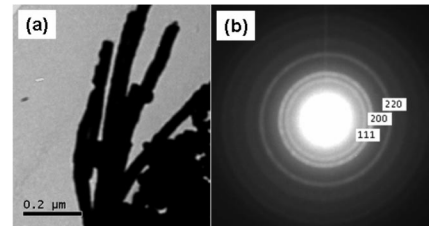


**Figure 2.** (a) TEM image of Y-junction platinum nanostructures after etching the alumina membrane; the SAED pattern (b) taken from a single Y-junction reveals that the structure is polycrystalline in nature.

Figure 2a shows the bright-field transmission electron micrograph (TEM) of such a Y-junction nanostructure, after removing the structures from the template. Y-junctions reveal the stem and branches having diameter in complete agreement with the SEM results. Figure 2b shows the selected area electron diffraction (SAED) taken from a single Y-junction, where the ring pattern demonstrates that the structure is polycrystalline in nature with (111), (200), (220), and (311) planes, could be

(11) (a) Li, J.; Papadopoulos, C.; Xu, J. *Nature* **1999**, *402*, 253. (b) Meng, G.; Jung, Y. J.; Cao, A.; Vajtai, R.; Ajayan, P. M. *Proc. Natl. Acad. Sci.* **2005**, *102*, 7074.

(12) (a) Gao, T.; Meng, G.; Zhang, J.; Sun, S.; Zhang, L. *Appl. Phys. A: Mater. Sci. Process.* **2002**, *74*, 403. (b) Choi, J.; Sauer, G.; Nielsch, K.; Wehrspohn, R. B.; Gošele, U. *Chem. Mater.* **2003**, *15*, 776.

(13) Singh, K. V.; Martinez-Morales, A. A.; Andavan, G. T. S.; Bozhilov, K. N.; Ozkan, M. *Chem. Mater.* **2007**, *19*, 2446.

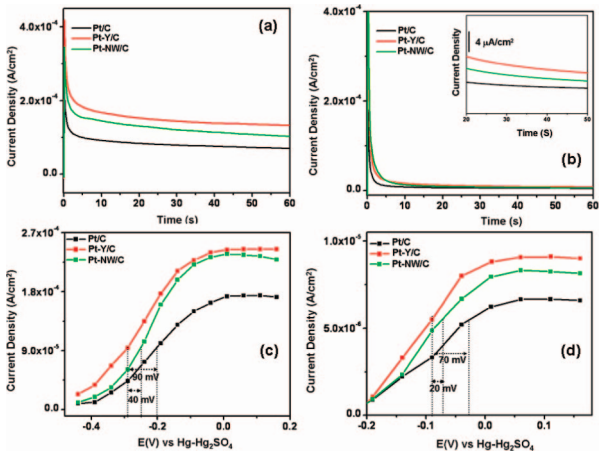


**Figure 3.** Comparison of electrocatalytic activity of Pt-Y/C, Pt-NW/C, and Pt/C. (a, b) Transient current density curves of formic acid (at –0.24 V) and ethanol oxidation (at –0.04 V), inset shows the enlarged view; (c, d) potential-dependent steady-state current density for both formic acid and ethanol oxidation reactions.

indexed to the face-centered cubic (fcc) structure of Pt.[14] Similarly, powder X-ray diffraction patterns (not shown for brevity) of these structures also match well with the Bragg reflections of the standard and phase-pure fcc structure of Pt; the crystallite size calculated using the Scherrer formula is ca. 9.2 nm, considering (111) reflections.

To explore the catalytic activity of these Y-shaped platinum nanostructures, we have investigated their utility for the electro-oxidation of formic acid and ethanol, which are two promising reactants for direct type of microfuel cells. Accordingly, (Figure 3a.) shows a comparison of transient current density of formic acid oxidation at −0.24 V (potential selected from cyclic voltammogram) on the Pt/C (commercial platinized carbon), Pt-Y/C (Y-junction Pt nanostructure in vulcan XC −72 carbon) and Pt-NW/C (Pt nanowires in vulcan XC −72 carbon) at room temperature. The oxidation current has been normalized to electroactive Pt surface area ($A_{Pt}$) so that the current density ($j$) can be directly used to compare the catalytic activity of both the samples. Interestingly, the oxidation current density on Pt-Y/C is significantly higher compared to that on both Pt-NW/C and Pt/C and the enhancement factor $R$, which is defined as the ratio of the current density measured on Pt-Y/C versus that acquired on Pt-NW/C or Pt/C, varies from 270 to 120% for Pt/C and from 200 to 80% for the Pt-NW/C sample depending on the electrode potential. Furthermore, from the steady state $I-V$ plot (in which the steady-state current density is obtained from the current transients recorded for 60 s for various potentials, –0.44 to +0.16 V), we observe that at a given current density, the corresponding potential on Pt-Y/C is much lower than that for Pt-NW/C and Pt/C. Further, the value is shifted negatively by ca. 90 mV at a current density of $9.5 \times 10^{-5}$ A/cm$^2$ with respect to that of Pt/C, whereas the shift is ca. 40 mV as compared with Pt-NW/C. Recently Wang et al. have seen for tetrahexahedral platinum nanocrystals that at a given oxidation current density, these tetrahexahedra show a negative shift in potential by 60 mV compared to that on Pt/C catalyst toward formic acid oxidation, which is indeed significantly lower compared to that of Pt-Y nanostructures.[15]

Similar studies have been performed for ethanol oxidation, and the transient current density response of the three samples (Pt-Y/C, Pt-NW/C, and Pt/C) are shown in Figure 3b for comparison.

Interestingly, the transient current density on Pt-Y/C at −0.04 V is enhanced to 180% of that on the Pt/C and 130% of that on Pt-NW/C, and the enhancement factor varies between 180 and 120% in the potential region of −0.2 to 0.16 V for the Pt-C sample, whereas the factor varies from 130 to 90% for Pt-NW/C. Also from the potential-dependent current density curve (Figure 3d), it is obvious that the potential on Pt-Y/C is shifted negatively by 70 mV as compared to that of Pt/C, whereas a 20 mV shift with respect to that of Pt-NW/C occurs at the same current density of $5.5 \times 10^{-6}$ A/cm.$^2$ Hence, the Pt-Y nanostructures exhibit much enhanced catalytic activity per unit surface area for the oxidation of formic acid and ethanol. This could be perhaps due to the high density of active sites on the surface of Y-junction Pt (large surface area is expected for these high-aspect-ratio nanostructures), and in addition, it is presumed that the branched regions also enhance the activity because of a large field gradient. This is clearly obvious on comparison of the performance of both Y-junctions and linear structures (nanowires) of Pt. Further studies are essential to understanding the reason for the enhanced catalytic activity.

In summary, the use of a hierarchically designed template of porous anodic alumina membrane enables the fabrication of Y-junction nanostructures of platinum (possessing stem and branches having diameter 100 and 50 nm, respectively, and the angle between the branches is almost 12°). These structures exhibit enhanced electrocatalytic activity for the oxidation of formic acid (up to 270%) and ethanol (up to 180%) compared to that of Pt/C, whereas with respect to Pt-NW/C, the enhancement is up to 200% for formic acid and up to 130% for ethanol oxidation, which are of relevance to fuel cell technology. Moreover, the potential on Y-junction platinum is shifted negatively by ca. 90 mV as compared with Pt/C, whereas the shift is ca. 40 mV with respect to Pt-NW/C at the same current density. Similarly, for ethanol oxidation, the negative shift is 70 and 20 mV with respect to Pt/C and Pt-NW/C, respectively. The present method of fabrication of Y-junction nanostructures using hierarchical alumina templates could be extended to other metallic/semiconducting systems because this morphology provides great opportunities for the development of various fields including nanoelectronics.

**Acknowledgment.** A part of SEM studies were performed in the EPIC facility of NUANCE Center at Northwestern University. We thank CSIR (NMITLI Cell) for funding.

**Supporting Information Available:** Experimental details; SEM of Pt Y-junction and FESEM of Pt nanowires; cyclic voltammograms of formic acid and ethanol oxidation (PDF). This information is available free of charge via the Internet at http://pubs.acs.org.

CM702102B

(14) Yee, C.; Scotti, M.; Ulman, A.; White, H.; Rafailovich, M.; Sokolov, J. *Langmuir* **1999**, *15*, 4314.

(15) Tian, N.; Zhou, Z.-Y.; Sun, S.-G.; Ding, Y.; Wang, Z. L *Science* **2007**, *316*, 732.